ELSEVIER

Journal of Process Control 10 (2000) 209–218

JOURNAL OF PROCESS CONTROL

www.elsevier.com/locate/jprocont

Nonlinear model-based control of a batch reactive distillation column

Lalitha S. Balasubramhanya [a], Francis J. Doyle III [b,*]

[a] School of Chemical Engineering, Purdue University, West Lafayette, IN, USA
[b] Department of Chemical Engineering, University of Delaware, Newark DE, 19716, USA

Abstract

The inherent trade off between model accuracy and computational tractability for model-based control applications is addressed in this article by the development of reduced order nonlinear models. Traveling wave phenomena is used to develop low order models for multicomponent reactive distillation columns. A motivational example of batch esterification column is used to demonstrate the synthesis procedure. Tight control of the column is obtained with the use of reduced model in a model predictive control algorithm.

Keywords: Batch reactive distillation; Nonlinear MPC; Traveling waves

1. Introduction

The concept of combining reaction with distillation had been recognized as far back as 1920 [1]. However, it was not realized in practice until the last couple of decades when a few commercial reactive distillation columns were built. Reactive distillation is potentially attractive whenever conversion is limited by reaction equilibrium. The reaction must be carried out with an excess of one reactant to overcome the limitation resulting in large recycle costs. A reactive distillation can, however, be operated close to stoichiometric feed conditions. By distilling one of the products, the forward reaction can be favored to increase conversion. Since a catalyst is generally used to carry out the conversion, unwanted reactions can be suppressed by suitable choice of catalysts resulting in lower separation costs. Reactive distillation can also be used in distilling azeotropic mixtures. Some of the components can be forced to react resulting in a simplified phase behavior. Examples of commercial success in implementing the principles of reactive distillation include Nylon 6,6 process, Methyl Acetate process, and Methyl *tert*-Butyl Ether process [1].

However, in spite of the numerous studies conducted on understanding the fundamental thermodynamics and kinetics in the operation of the columns (e.g. [2–6]), very little work has been reported on the control of reactive distillation columns. Steady-state model analysis (e.g. [7–11]) as well as steady-state multiplicities (e.g. [12–14]) have been considered in detail by many researchers. Dynamic modeling and simulation have also been studied by (e.g. [15–18]). For batch reactive distillation columns, Cuille and Reklaitis [19] designed an efficient numerical simulation strategy while Reuter et al. [20] and Sørenson and Skogestad [21] have analyzed various control strategies. Wajge and Rekalitis [22,23] have proposed an efficient campaign structure for optimizing reactive batch distillation operation. Kumar and Daoutidis [24] presented a differential-algebraic-equation framework to control continuous reactive distillation columns. They also designed a nonlinear input–output linearizing controller for an ethylene glycol reactive distillation column that exhibited steady-state multiplicities as well as non-minimum phase behavior [25]. A Dynamic Matrix Control algorithm for startup and continuous operation of a reactive distillation column has also been proposed by Baldon et al. [26]. Though great strides have been made in understanding the behavior of reactive distillation columns, control of these columns is still an open research area. In this work, we will emphasize a model-based control approach to the problem.

Process models are an integral component of most computer integrated process operations [27]. Control schemes, optimization, process scheduling, fault diagnosis

* Corresponding author. Tel.: +1-302-831-0760; fax: +1-302-831-0457.
E-mail address: fdoyle@udel.edu (F.J. Doyle III).

0959-1524/99/$ - see front matter
PII: S0959-1524(99)00024-4

— all rely heavily on the process description. Independent of the specific design technique employed, the majority of the process controllers are based on some form of model describing the dynamic behavior of the process — be it just the process gain and the settling time, or systems of partial differential equations [28]. Models developed from first principles are a good source of process information, however, they are invariably complex, coupled, nonlinear partial differential equations. Numerical methods such as finite differences and orthogonal collocation can be used to simplify these equations, but they lead to a large number of ordinary differential equations. Hankel reduction, balanced realization and other techniques can be used for reducing the order of the equations but the resulting equations do not retain their physical significance. Understanding the physical significance of parameters and variables is often essential in developing an effective control strategy. This has fueled the need for low order nonlinear models that can capture the essential nonlinearity of the system while retaining mathematical simplicity as well as physical significance.

The approach taken in this paper is to develop low order nonlinear models to capture the essential nonlinear dynamic transport behavior of processes. Systems with distributed parameters often exhibit dynamic phenomena which resemble traveling waves. Conservation of mass, energy and momentum often results in traveling waves which can be represented by wave fronts, wave pulses and wave trains [29–31]. In chemical engineering, the propagation of waves has been studied extensively in connection with reaction engineering, combustion technology and separation processes. Examples include temperature and composition profiles in high-purity distillation columns [29,32], temperature profiles in fixed bed reactors [33,34] and compositions profiles in adsorption columns [35–37]. Low order models can then be used in model based control strategies [38–42] to achieve tight control of the processes.

An esterification process is used to motivate the development of low order models for reactive distillation columns. In Section 2, the case study is described in detail. In Section 3, the steps in developing a reduced model based on the traveling wave, phenomenon are outlined. The validation of the reduced model is presented in Section 4 and control of the process using the reduced model is presented in Section 5.

2. Batch reactive distillation column case study

The case study is an esterification process where *Ethanol* reacts with *Acetic Acid* to produce *Ethylacetate* and *Water*:

$$C_2H_5OH + CH_3COOH \rightleftharpoons CH_3COOC_2H_5 + H_2O$$

The reaction kinetics are given by $R = k_1\tilde{x}_2\tilde{x}_0 - k_2\tilde{x}_1\tilde{x}_3$ where $\tilde{x}$ are the liquid mole fractions and k_1 and k_2 are the reaction rate constants. The components are numbered as follows: Acetic Acid (0) < Water (1) < Ethanol (2) < Ethylacetate (3). Constant relative volatility is assumed to represent the VLE. Using *Acetic Acid* as the reference, the relative volatilities of the components can be calculated:

$$\alpha_0 = 1 < \alpha_1 = 1.72 < \alpha_2 = 3.9281 < \alpha_3 = 4.0286 \qquad (1)$$

The product of interest is *Ethylacetate* and the objective is to push the reaction in the forward direction and increase the yield of *Ethylacetate*. The operation under consideration is a batch reactive distillation column consisting of eight trays. For simulation purposes, the process is modeled using a tray-by-tray description resulting in thirty-one differential equations. The specific balances are:

$$M_j\frac{d\tilde{x}_{i,j}}{dt} = L\tilde{x}_{i,j+1} + V\tilde{y}_{i,j-1} - L\tilde{x}_{i,j} - V\tilde{y}_{i,j} + \varepsilon_i M_j R$$

$$i = 0, 2, 3 \text{ (components)} \quad j = 1, ..., 8 \text{ (trays)}$$

$$M_9\frac{d\tilde{x}_{i,9}}{dt} = V\tilde{y}_{i,8} - L\tilde{x}_{i,9} - D_{dis}\tilde{x}_{i,9} + \varepsilon_i M_9 R$$

$$i = 0, 2, 3 \text{ (condenser)}$$

$$\frac{d\left(M_0\tilde{x}_{i,0}\right)}{dt} = L\tilde{x}_{i,1} - V\tilde{y}_{i,0} + \varepsilon_i M_0 R \quad i = 0, 2, 3 \text{ (reboiler)}$$

$$\frac{dM_0}{dt} = L - V \text{ (reboiler)}$$

$$\tilde{x}D_{c,j} = 1 - \sum_{i=A_c}^{C_c}\tilde{x}_{i,j} \quad j = 0, 1, ..., 9$$

$$\tilde{y}_{i,j} = \frac{p_{i,j}\left(T_j, \tilde{x}_{i,j}\right)}{P_j} \quad i = 0, 1, 2, 3 \quad j = 0, 1, ..., 9$$

$$\sum_{i=A_c}^{D_c}\tilde{y}_{i,j} = \sum_{i=A_c}^{D_c}\frac{p_{i,j}\left(T_j, \tilde{x}_{i,j}\right)}{P_j} = 1 \quad j = 0, 1, ..., 9 \qquad (2)$$

The trays and the condenser are assumed to have constant molar overflow. D_{dis} is the distillate flow collected at the condenser which is the product of interest. ε_i, the stoichiometric coefficient, is 1 for Ethylacetate and Water, and is -1 for Ethanol and Acetic Acid. The partial vapor pressure ($p_{i,j}$) and the vapor composition ($\tilde{y}_{i,j}$) is calculated using Antoine's constants. $\tilde{x}_{i,j}$ is the liquid mole fraction of component i on plate j and M_j is the molar holdup on plate j. The values of the parameters used in

simulating the detailed column are presented in Table 1. For a known pressure (P_j) drop in the column, the compositions and the temperature are iteratively calculated to satisfy the mole balances. This essentially assumes that the thermal equilibrium is attained and the equilibrium temperature depends only on the pressure and composition. It should be noted that further detail can be introduced in the model (hydrodynamics, energy balances, etc.), resulting in a complex model of higher order.

For the purposes of analysis, a spatial distribution of the components is considered. Based on the constant relative volatility description of the vapor-liquid-equilibrium (VLE), the vapor compositions can be represented as ($j = 0, 1, 2, 3$):

$$\tilde{y}_j = \frac{\alpha_j \tilde{x}_j}{(\alpha_1 - 1)\tilde{x}_1 + (\alpha_2 - 1)\tilde{x}_2 + (\alpha_3 - 1)\tilde{x}_3 + 1}$$

The reboiler generates a vapor phase which acts as the feed to the distillation column. For the following theoretical development, we consider a continuous column versus a set of discrete trays. The distribution of the various species in the distillation column can then be represented by the following partial differential equations (mass balances):

Table 1
Detailed column parameters

Holdup (kmols)	
$M_{0_{\text{init}}}$	4.7980
M_j $(j = 1, ..., 8)$	0.0125
M_9	0.1

Reaction constants (litre/gmol min)	
k_1	2900 exp(−7150/T(K))
k_2	7380 exp (−7150/T(K))

Vapor pressure (torr); $\log_{10}(P) = A_P - \dfrac{B_p}{T(^\circ C) - C_p}$

Components	Antoine's constants		
	A_p	B_p	C_p
Acetic acid	8.02100	1936.010	258.451
Ethanol	8.11220	1592.864	226.184
Ethylacetate	7.10179	1244.951	217.881
Water	8.07131	1730.630	233.426

Density (g/cc) $\rho_l = A_d B_d^{-(1-T_r)^{2/7}}$; $T_r = T(\text{K})/T_c(\text{K})$

Components	A_d	B_d	T_c(K)
Acetic acid	0.3512	0.2	594.4
Ethanol	0.2903	0.2760	516.2
Ethylacetate	0.3084	0.252	523.2
Water	0.3471	0.274	647.3

$$\begin{aligned}
\frac{\partial \tilde{x}_1}{\partial t} - \frac{\partial \tilde{x}_1}{\partial z} + \nu \frac{\partial \tilde{y}_1}{\partial t} + \mu \frac{\partial \tilde{y}_1}{\partial t} &= R \\
\frac{\partial \tilde{x}_2}{\partial t} - \frac{\partial \tilde{x}_2}{\partial z} + \nu \frac{\partial \tilde{y}_2}{\partial t} + \mu \frac{\partial \tilde{y}_2}{\partial t} &= -R \\
\frac{\partial \tilde{x}_3}{\partial t} - \frac{\partial \tilde{x}_3}{\partial z} + \nu \frac{\partial \tilde{y}_3}{\partial t} + \mu \frac{\partial \tilde{y}_3}{\partial t} &= R
\end{aligned} \tag{3}$$

where

$$R = k_1 \tilde{x}_2 (1 - \tilde{x}_1 - \tilde{x}_2 - \tilde{x}_3) - k_2 \tilde{x}_1 \tilde{x}_3 \tag{4}$$

$$\tilde{x}_0 = 1 - \tilde{x}_1 - \tilde{x}_2 - \tilde{x}_3$$

R describes the rate of generation of the components, $\nu(= 0.01)$ is the ratio of the vapor to liquid holdup, and $\mu = \dfrac{V}{L}$ is the ratio of the vapor to the liquid flow rates. Since the mole fractions sum up to 1, $\tilde{x}_0 = 1 - \sum_{j=1}^{3} \tilde{x}_j$. Eq. (3) is a continuous representation of the discrete set of equations for the column without the reboiler. These equations can be analyzed to demonstrate the formation of shock waves [43].

3. Low order model development

In the derivation of the reduced model the following simplifications are introduced:

- components with similar relative volatilities are lumped together;
- reaction equilibrium is assumed;
- a constant spatial structure for the composition profile of $\tilde{x}_3$ is assumed; and
- a constant spatial structure for the temperature profile is assumed.

The relative volatilities of *Ethanol* ($\alpha_2 = 3.9281$) and *Ethylacetate* ($\alpha_3 = 4.0286$) are very close to each other indicating similar vapor-liquid-equilibrium. Thus, the mole fractions of the two components can be lumped together. Similarly, the relative volatilities of *Water* ($\alpha_1 = 1.72$) and *Acetic Acid* ($\alpha_0 = 1$) are relatively close and their mole fractions can be lumped together as well. We define the new variables:

$$\tilde{x}_{l_1} = \tilde{x}_3 + \tilde{x}_2 \tag{5}$$

$$\tilde{x}_{l_2} = \tilde{x}_1 + \tilde{x}_0 = 1 - \tilde{x}_{l_1} \tag{6}$$

Let the relative volatility of $\tilde{x}_{l_1}$ with respect to $\tilde{x}_{l_2}$ be given by α_l, then the vapor composition is given by

$$\tilde{y}_{l_1} = \frac{\alpha_l \tilde{x}_{l_1}}{(\alpha_l - 1)\tilde{x}_{l_1} + 1} \tag{7}$$

$$\tilde{y}_{l_2} = \frac{\tilde{x}_{l_2}}{(\alpha_l - 1)\tilde{x}_{l_1} + 1} = 1 - \tilde{y}_{l_1} \tag{8}$$

α_l is the average relative volatility and for this case it is computed to be 2.9253. Using the lumping simplification, Eq. (3) is reduced to

$$\frac{\partial \tilde{x}_{l_1}}{\partial t} - \frac{\partial \tilde{x}_{l_1}}{\partial z} + \nu \frac{\partial \tilde{y}_{l_1}}{\partial t} + \frac{V}{L}\frac{\partial \tilde{y}_{l_1}}{\partial t} = 0 \tag{9}$$

The equilibrium relation is given by Eq. (7), $\tilde{x}_{l_2} = 1 - \tilde{x}_{l_1}$, and $\tilde{y}_{l_2} = 1 - \tilde{y}_{l_1}$. Lumping of the components leads to a pseudo-binary distillation column which can be analyzed for the formation of shock waves. The VLE relation is used to show that

$$\frac{\mathrm{d}^2 \tilde{y}_{l_1}}{\mathrm{d}\tilde{x}_{l_1}^2} = -\frac{\alpha_l(\alpha_l - 1)}{\left((\alpha_l - 1)\tilde{x}_{l_1} + 1\right)^3} < 0 \tag{10}$$

Since $\dfrac{\mathrm{d}^2 \tilde{y}_{l_1}}{\mathrm{d}\tilde{x}_{l_1}^2} < 0$, the characteristics for the Eq. (9) overlap which results in the formation of shock waves. The system travels with a shock velocity given by

$$\lambda_{\mathrm{sh}} = \frac{-1 + \mu \dfrac{\left[\tilde{y}_{l_1}\right]}{\left[\tilde{x}_{l_1}\right]}}{1 + \nu \dfrac{\left[\tilde{y}_{l_1}\right]}{\left[\tilde{x}_{l_1}\right]}} \tag{11}$$

where [.] represents a jump in the quantity across the shock.

Using a second order approximation for the VLE, Marquardt and Gilles [42] analytically derived a function to describe the shape of the composition profile for an ordinary binary distillation column. A similar expression is used to approximate the concentration profile of the lumped system:

$$\tilde{x}_{l_1}(z) = \tilde{x}_{l_{\min}} + \frac{\tilde{x}_{l_{\max}} - \tilde{x}_{l_{\min}}}{1 + \exp(-\gamma_l(\xi - \xi_s))} \tag{12}$$

where $\tilde{x}_{l_{\min}}$ and $\tilde{x}_{l_{\max}}$ are the constants determining the boundary of the concentration profiles and γ_l reflects the steepness of the profile. $\xi = z - \lambda_l t$, and ξ_s represents the stagnation or the inflection point of the profile. The time derivative of this stagnation point is given by the shock velocity in Eq. (11). The dynamics of the stagnation point can be linked back to the shock velocity given by Eq. (11) as follows:

$$\frac{\mathrm{d}\xi_s}{\mathrm{d}t} = \lambda_l = \frac{-1 + \mu \dfrac{\left[\tilde{y}_{l_1}\right]}{\left[\tilde{x}_{l_1}\right]}}{1 + \nu \dfrac{\left[\tilde{y}_{l_1}\right]}{\left[\tilde{x}_{l_1}\right]}} \tag{13}$$

Thus, from Eqs. (11) and (12) the distribution of $\tilde{x}_{l_1}$, along the column, and its dynamic behavior, can be obtained.

The second assumption employed in this development was that reaction equilibrium is attained. This is consistent with the analysis of [2,3] and occurs, for example, in the limit of excess catalyst.

This results in the following relationship between the components:

$$K_r = \frac{k_1}{k_2} = \frac{\tilde{x}_3 \tilde{x}_1}{\tilde{x}_2 \tilde{x}_0} \tag{14}$$

Using the reaction equilibrium assumption the composition of component (1) can be represented as

$$\begin{aligned}\tilde{x}_1 &= \frac{k_1\tilde{x}_2 - k_1\tilde{x}_2{}^2 - k_1\tilde{x}_3}{k_1\tilde{x}_2 + k_2\tilde{x}_3} \\ &= \frac{k_1\left(\tilde{x}_{l_1} - \tilde{x}_3\right) - k_1\tilde{x}_{l_1}{}^2 + k_1\tilde{x}_3\tilde{x}_{l_1}}{k_1\tilde{x}_{l_1} + (k_2 - k_1)\tilde{x}_3}\end{aligned} \tag{15}$$

Also $\tilde{x}_2 = \tilde{x}_{l_1} - \tilde{x}_3$ and $\tilde{x}_0 = 1 - \tilde{x}_1 - \tilde{x}_{l_1}$. Thus, the mole fractions of all the components can be represented as functions of $\tilde{x}_3$ and $\tilde{x}_{l_1}$. Since the distribution of $\tilde{x}_{l_1}$ is given by Eq. (12), the only component of interest is $\tilde{x}_3$.

The distribution of $\tilde{x}_3$ can be obtained from Eq. (3)

$$\frac{\partial \tilde{x}_3}{\partial t} + \nu \frac{\partial \tilde{y}_3}{\partial t} - \frac{\partial \tilde{x}_3}{\partial z} + \mu \frac{\partial \tilde{y}_3}{\partial z} = 0 \tag{16}$$

The right hand side of Eq. (3) is identically zero as reaction equilibrium is assumed. Assuming VLE is attained, we get

$$\begin{aligned}&\left(1 + \nu\left[\frac{\partial \tilde{y}_3}{\partial \tilde{x}_3}\right]\tilde{x}_{l_1}\right)\frac{\partial \tilde{x}_3}{\partial t} + \left(-1 + \mu\left[\frac{\partial \tilde{y}_3}{\partial \tilde{x}_3}\right]\tilde{x}_{l_1}\right)\frac{\partial \tilde{x}_3}{\partial z} \\ &= (\nu\lambda_l - \mu)\left[\frac{\partial \tilde{y}_3}{\partial \tilde{x}_{l_1}}\right]\tilde{x}_3\frac{\mathrm{d}\tilde{x}_{l_1}}{\mathrm{d}\xi}\end{aligned} \tag{17}$$

The characteristics for the above partial differential equation indicate the formation of shock waves. Details of the analysis can be obtained from [43]. Thus, the reduced model is able to capture the formation of shocks.

Since the partial differential equation for $\tilde{x}_3$ admits shock, the composition profile travels with a shock velocity. Also, as the concentrations of the species are interlinked via the VLE, all the composition profiles travel with the same wave velocity. This shock velocity can be represented as:

$$\lambda_{\mathrm{sh}} = \frac{-1 + \mu \dfrac{\left[\tilde{y}_j\right]}{\left[\tilde{x}_j\right]}}{1 + \nu \dfrac{\left[\tilde{y}_j\right]}{\left[\tilde{x}_j\right]}} \quad j = 1, 2, 3 \tag{18}$$

It is assumed that the structure of the composition profile of $\tilde{x}_3$ remains constant and can be represented as:

$$\tilde{x}_3 = \tilde{x}_{3_{\min}} + \frac{\tilde{x}_{3_{\max}} - \tilde{x}_{3_{\min}}}{1 + \exp(-\gamma_3(\xi - \xi_s))} \tag{19}$$

This structure is similar to the structure derived theoretically by Marquardt and Gilles [42] [Eq. (12)]. It is assumed that the structure obtained from a second order approximation to VLE can be used to model the profile of component $\tilde{x}_3$. $\tilde{x}_{3_{\min}}$ and $\tilde{x}_{3_{\max}}$ fix the end points of the profile while γ_3 gives the steepness of the profile.

The energy balances are intrinsically linked to the mass balances in a column and hence traveling composition profiles imply traveling temperature profiles. As was explained earlier, for a given pressure drop, fixing the temperature fixes the composition and vice versa. The relationship is based on the vapor liquid equilibrium (relative volatility or the Antoine's equations). Since the temperature is closely related to the composition profiles, a constant structure for the temperature profile is assumed:

$$T_m = T_{m_{\min}} + \frac{T_{m_{\max}} - T_{m_{\min}}}{1 + \exp\left(-\gamma_{T_m}(\xi - \xi_s)\right)} \tag{20}$$

where, as before, $T_{m_{\max}}$ and $T_{m_{\min}}$ fix the end points of the profile while γ_{T_m} gives the "steepness" of the profile. This is equivalent to assuming that energy balances reach steady state faster than the mass balances. The temperature profile also travels with the shock velocity given by Eq (18).

To summarize, the reduced model consists of the following components:

- mass balance equations (four differential equations) to analyze the dynamics of the reboiler
- distribution of $\tilde{x}_{l_1}$ is given by Eq. (12)
- distribution of $\tilde{x}_3$ is given by Eq. (19)
- $\tilde{x}_2 = \tilde{x}_{l_1} - \tilde{x}_3$, $\tilde{x}_1 = \dfrac{k_1\tilde{x}_2 - k_1\tilde{x}_2^2 - k_1\tilde{x}_3}{k_1\tilde{x} + k_2\tilde{x}_3}$, and $\tilde{x}_0 = 1 - \tilde{x}_1 - \tilde{x}_{l_1}$
- the temperature profile for the system is given by Eq. (20)
- the velocity with which the waves travel is given by

$$\lambda_{\text{sh}} = \frac{-1 + \mu\dfrac{[\tilde{y}_3]}{[\tilde{x}_3]}}{1 + \nu\dfrac{[\tilde{y}_3]}{[\tilde{x}_3]}}$$

Thus, a total number of five differential equations and six algebraic equations are needed to represent the reduced model, compared with 31 differential equations and 10 algebraic equations in the original (full) model.

4. Open-loop model validation

In this section, the dynamic behavior of the detailed column is compared to both the nonlinear reduced model and a linear model. In practice, it is difficult to obtain the composition measurements at frequent time intervals to perform feedback control. Hence, temperature measurements are used as the secondary output for control purposes. In a typical distillation column the regions of intense mass transfer are located in the middle of the column while the ends of column are used for purification. These regions are more sensitive to disturbances and inputs compared to the ends of columns. Similar behavior is observed in the reactive distillation column under discussion. Hence, the temperature on tray 2, which is one of the most sensitive to the changes in the column, is used as the secondary output in this study. The inputs to the system are the liquid flow rate, L, and the vapor flow rate, V.

The detailed column can represented as a 31st order nonlinear state-space model:

$$\dot{\boldsymbol{x}} = \boldsymbol{f}(\boldsymbol{x}, \boldsymbol{u}) \tag{21}$$

$$y = h(\boldsymbol{x}, \boldsymbol{u})$$

where $\boldsymbol{x}$ are the 31 states of the system, $\boldsymbol{f}(\boldsymbol{x}, \boldsymbol{u})$ defines the dynamics of the system, $\boldsymbol{u}$ is the input to the system, and y is the output. The column can be linearized around the initial operating point to obtain a linear model.

$$\dot{\boldsymbol{x}} = \boldsymbol{f}(\boldsymbol{x}_0, \boldsymbol{u}_0) + A(\boldsymbol{x} - \boldsymbol{x}_0) + B(\boldsymbol{u} - \boldsymbol{u}_0) \tag{22}$$

$$y = h(\boldsymbol{x}_0, \boldsymbol{u}_0) + C(\boldsymbol{x} - \boldsymbol{x}_0) + D(\boldsymbol{u} - \boldsymbol{u}_0)$$

Here, $A = \dfrac{\mathrm{d}\boldsymbol{f}}{\mathrm{d}\boldsymbol{x}}$, $B = \dfrac{\mathrm{d}\boldsymbol{f}}{\mathrm{d}\boldsymbol{u}}$, $C = \dfrac{\mathrm{d}h}{\mathrm{d}\boldsymbol{x}}$, $D = \dfrac{\mathrm{d}h}{\mathrm{d}\boldsymbol{u}}$, $\boldsymbol{x}_0$ and $\boldsymbol{u}_0$ are the initial states and inputs, and $\boldsymbol{f}(\boldsymbol{x}_0, \boldsymbol{u}_0)$ and $h(\boldsymbol{x}_0, \boldsymbol{u}_0)$ are functions evaluated at the initial conditions. Typically the detailed column is linearized at a steady state operating point and $\boldsymbol{f}(\boldsymbol{x}_0, \boldsymbol{u}_0) = 0$. However, a batch distillation column is operated at an unsteady state operating point and $\boldsymbol{f}(\boldsymbol{x}_0, \boldsymbol{u}_0) \neq 0$. This adds a constant bias to the usual linear model based on the Jacobian and plays an important role in the dynamics of the system. The third model under consideration is the nonlinear wave model discussed in the previous section, which can be represented as a 5th order nonlinear state-space model:

$$\dot{\boldsymbol{x}}_r = \boldsymbol{f}_r(\boldsymbol{x}_r, \boldsymbol{u}) \tag{23}$$

$$y_r = h_r(\boldsymbol{x}_r, \boldsymbol{u})$$

where $\boldsymbol{x}_r$ are the five states of the reduced model, $\boldsymbol{u}$ is the input to the system, $\boldsymbol{f}_r$ defines the dynamics of the

reduced model, and h_r defines the output of the reduced model. In this case, the differential equations consist of the mass balances for the reboiler and the equation defining the shock dynamics of the traveling wave [Eq. (18)]. The parameters defining the reduced model are presented in Table 2.

The initial flow rates in the column are $L = 2.15$ kmols/h and $V = 2.3$ kmols/h. As a batch column is never truly at steady state, the system evolves with time even if the inputs are maintained at the initial flow rates. The measured outputs (temperature of tray 2) from the three models are compared in Fig. 1. The nonlinear model (dashed line) outperforms the linear model (dotted line) in predicting the dynamic behavior of the detailed column (solid line). The traveling waves in the detailed column are compared to the traveling waves in the reduced model in Fig. 2. The temperature profiles along the length of the column are plotted at different instances of time. The reduced model is qualitatively able to capture the traveling wave phenomenon exhibited by the detailed column. The normalized distance of tray 2 from the reboiler is equal to 0.22. Composition profiles can also be obtained at the time instances. The reduced model again qualitatively captures the behavior of the detailed column (Fig. 3). As would be expected with an approximate modeling scheme, there is some quantitative deterioration of the model fidelity.

Table 2
Wave model parameters

Parameters	Numerical values
ν	0.01
α_3	4.0286
α_2	3.9281
α_1	1.72
α_0	1.0
$\tilde{x}_{l_{\min}}$	0.15
$\tilde{x}_{l_{\max}}$	1.0
γ_l	8.8
$\tilde{x}_{3_{\min}}$	0.025
$\tilde{x}_{3_{\max}}$	0.65
γ_3	10.0
$T_{m_{\min}}$	372.0
$T_{m_{\max}}$	250.5
γ_{T_m}	10.5

5. Controller design

The control methodology for the batch column is based on model predictive control (MPC). MPC as a control methodology has gained tremendous importance in recent years and has been implemented with

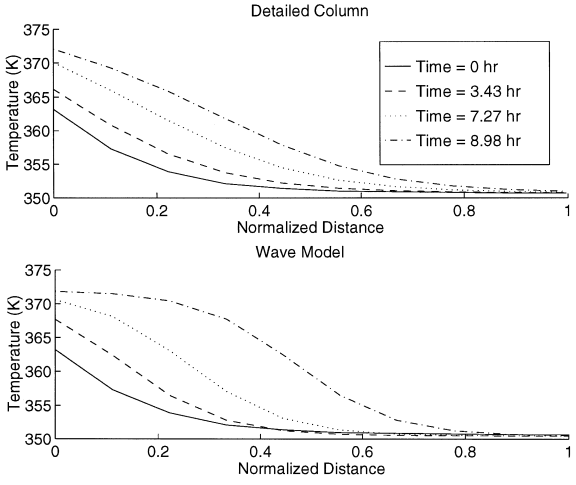

Fig. 2. Open-loop response of traveling temperature profiles in the detailed model and the nonlinear wave model ($\boldsymbol{u} = [2.15\ 2.3]^T$ kmol/h).

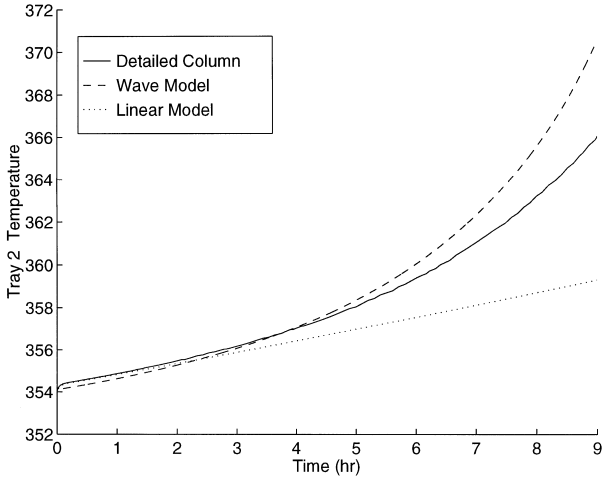

Fig. 1. Comparison of tray temperatures between detailed column, nonlinear wave model, and linear model for $\boldsymbol{u} = [2.15\ 2.3]^T$ kmol/h.

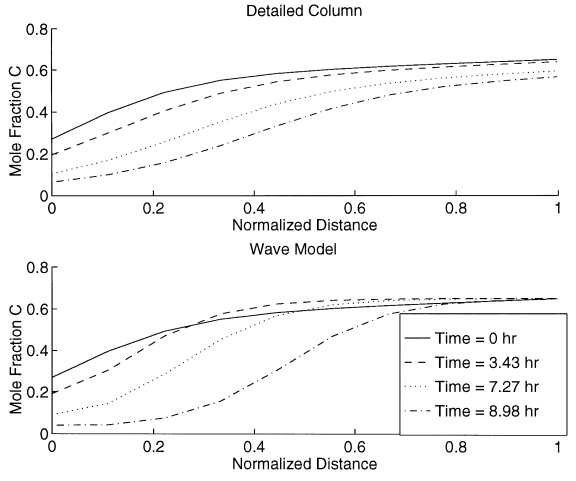

Fig. 3. Open-loop response of traveling composition profiles in the detailed column and the nonlinear wave model ($\mathbf{u} = [2.15\ 2.3]^T$ kmol/h).

great success in the industry [44]. Most MPC algorithms are based on linear models such as step or impulse response models. However, in this work, a nonlinear process model is employed, necessitating the use of a nonlinear optimization program to minimize the objective function. Since this computation has to be completed on-line, it is necessary to choose a model that results in lower computational complexity. The model simplification may also obviate convergence issues that can be encountered with large scale nonlinear process models in optimization problems. The reduced order model developed earlier based on the traveling wave phenomenon is used as the simplified model to represent the column. The formulation of the control problem is a nonlinear modification of the formulation suggested by Ricker [45]. In our formulation, the reduced wave model is used to predict outputs into the future and a nonlinear optimization routine (obtained from MATLAB) is used to calculate the input moves as well. Hence, the approach used is the Nonlinear Quadratic Dynamic Matrix Control with State Estimation (NLQDMC/SE).

The control objective is to obtain as pure a sample of the product over the entire batch as possible. It is difficult to obtain the composition of the product at every time step for feedback control. However, since the composition in the column is intimately linked to the temperature, the composition of the product can be inferentially controlled by controlling the temperature in the column. As discussed in the previous section, the temperature on tray 2 will be used as the controlled variable.

The objective function for the minimization problem to be solved at each instance of time is given by:

$$\min_{\boldsymbol{u}} \sum_{i=k}^{k+p} \left(r_{\mathrm{dis}}(i) - y_{\mathrm{dis}}(i)^2\right)$$

subject to the constraints:

$$\boldsymbol{u}(i) \geqslant 0.0 \qquad i = k, ..., k+m$$

$$\boldsymbol{u}(i) \leqslant \boldsymbol{u}_{\max} \qquad i = k, ..., k+m$$

$$T_{\mathrm{tray2}}(i) \leqslant T_{\max} \qquad i = k, ..., k+p$$

$$\Delta\boldsymbol{u}(i) \leqslant \Delta\boldsymbol{u}_{\max} \qquad i = k, ..., k+m$$

$$y_{\mathrm{dis}}(i) = y_{\mathrm{dis}}(i-1) + (V(i-1) - L(i-1))T_s$$

$$i = k, ..., k+p$$

$r_{\mathrm{dis}}(i)$ is the reference trajectory for the amount of distillate to be produced at time instant $k+i$, T_s, is the sample time (0.3 h), $y_{\mathrm{dis}}(i)$ is the predicted amount of distillate produced, $\boldsymbol{u}_{\max}$ is the maximum input, $\Delta\boldsymbol{u}_{\max}$ is the maximum input change at every time period, and $T_{\max}$ is the maximum temperature allowed on tray 2. $\boldsymbol{u}$ is a vector of magnitude $2m \times 1$ corresponding to the two inputs (vapor flow and liquid flow) and the m moves that the controller calculates at every time step. The temperature constraint at $T_{\max}$ places a lower bound on the purity of the distillate. $T_{\mathrm{tray2}}(i)$ is the output of the reduced model used to predict the temperature i steps into the future. A linear Kalman filter is used to update the states and the outputs of the reduced model based on the measurements of temperature obtained from the real column. In an effort to reduce computational load, more complex estimation schemes, such as a nonlinear observer, were not employed. A schematic of the controller design in presented in Fig. 4. The solid lines trace the control loop associated with the amount of distillate collected while the dashed lines trace the temperature feedback to the controller. The dotted line represents the MPC controller that minimizes the difference between the reference trajectory and the output prediction within the constraints imposed.

For a reference trajectory composed of a series of steps, the output of the condenser and the input moves are shown in Fig. 5. The model used to predict the temperature is the nonlinear wave model developed earlier. As shown, the output tracks the reference trajectory very closely. In Fig. 6, the output and the manipulated input moves when the detailed column is used in the controller is shown. On comparing Figs. 5 and 6, one can conclude that the reduced model does as well as the detailed column model in achieving the controller objectives. The advantage in using the reduced model is in the reduced computational effort. The closed-loop simulation time using the detailed column was 225.39 cpu s while the time required using the reduced model was 34.34 cpu s. Thus, the computational time can be reduced by a factor of about 6.5 by using the reduced model. All the simulations were carried

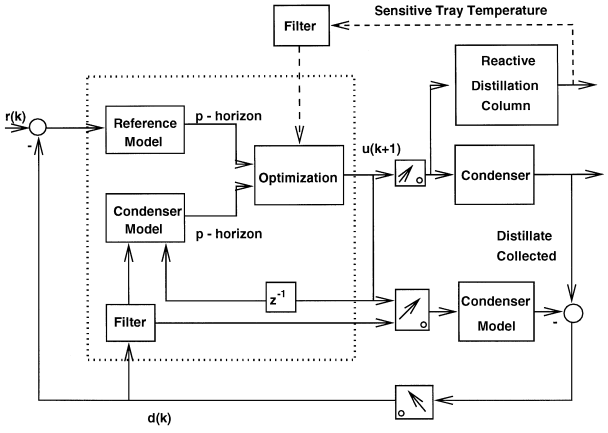

Fig. 4. Schematic diagram of MPC algorithm with temperature feedback.

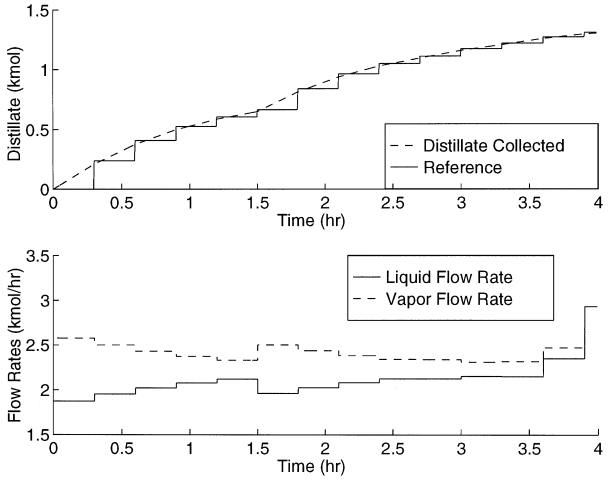

Fig. 5. Closed-loop response to filtered sequence of step changes in distillate reference (controller model = wave model).

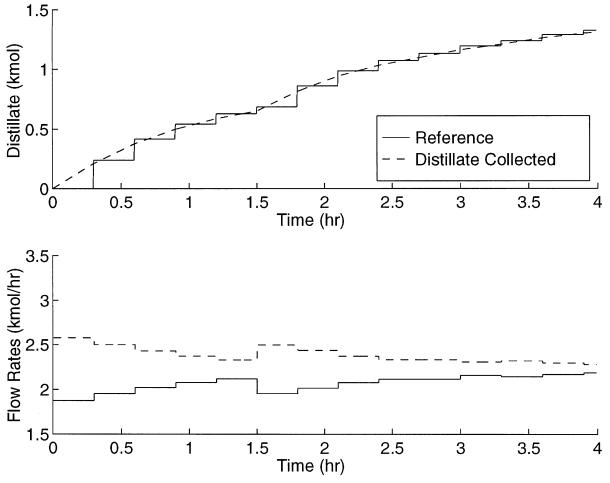

Fig. 6. Closed-loop response to filtered sequence of step changes in distillate reference (controller model = detail column model).

out on a Sun3000 workstation. For both the simulations $p = 2$, $m = 1$, $T_{\max} = 370$ K, $\boldsymbol{u}_{\max} = [3.8\ 4.00]^T$ kmol/h, and $\Delta\boldsymbol{u}_{\max} = [0.6\ 0.6]^T$ kmol/h.

The responses of the wave model (dashed line), detailed column (solid line), and the linear model (dashed dot) to the input moves from Fig. 5 are analyzed and shown in Fig. 7. As can be seen, the wave model significantly outperforms the linear model in capturing the dynamics of the detailed model. Next, the mole fraction of the product of interest, *Ethyl Acetate*, in the vapor stream exiting the column and the distillate collected is plotted in Fig. 8. Thus, by maintaining the temperature below a maximum temperature, the mole fraction of the product can be maintained above a certain value.

Finally, a ramp setpoint for the distillate is considered in Fig. 9. The model used for prediction in the controller is the nonlinear wave model. The output of the plant

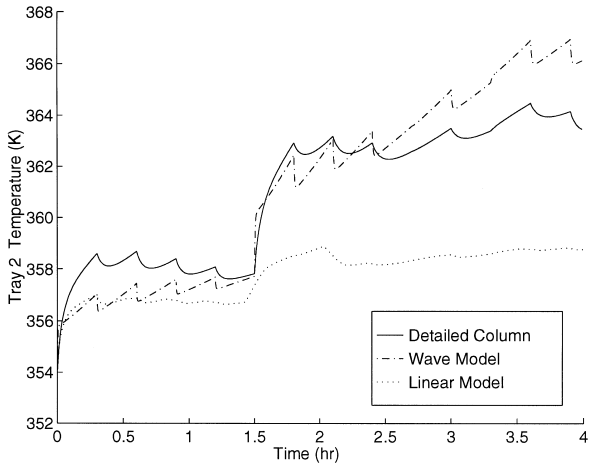

Fig. 7. A comparison of the temperature resposes of the detailed column, wave model, and the linear model to the manipulated input moves presented in Fig. 5.

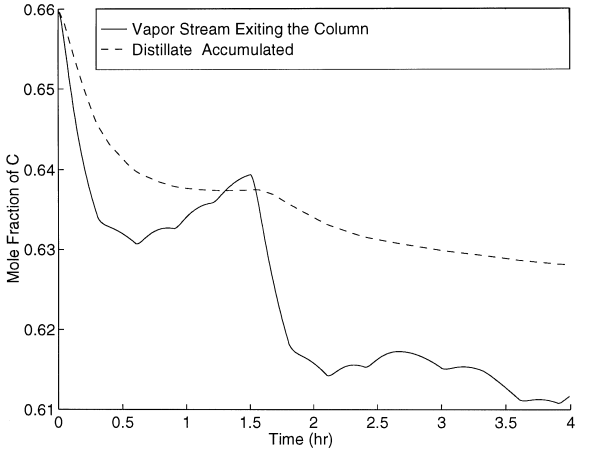

Fig. 8. The instantaneous mole fraction of Ethyl Acetate in the vapor stream and the distillate collected in response to the manipulated input moves shown in Fig. 5.

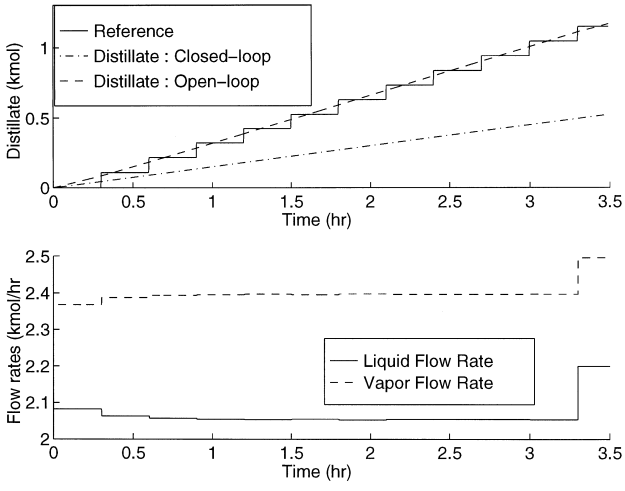

Fig. 9. The distillate collected closed-loop is compared to the reference trajectory and the distillate collected open-loop. The input moves of the controller are shown in the bottom plot. The input for the open-loop simulation is $\boldsymbol{u}$ $[2.15\ 2.3]^T$ kmol/h.

(dashed line) is compared to the reference trajectory (solid line). The amount of distillate collected in the absence of the controller (for input $\boldsymbol{u}_0 = [2.15\ 2.3]^T$) is shown as the dashed-dot line. Thus, it is seen that the amount of distillate produced can almost be doubled by appropriate control action. The input moves computed by the controller are given by the bottom plot in Fig. 9.

6. Conclusions

In this study, a reduced model for reactive distillation columns was developed based on the traveling wave phenomena. A motivating example of esterification was used to demonstrate the approach. The reduced model was obtained by introducing the following simplifications in the partial differential representation of the detailed model: (1) lumping of the components with similar VLE; (2) reaction equilibrium; (3) constant structure of the composition profiles; and (4) constant structure for the temperature profile. The reduced model consists of five differential equations — four to represent the dynamics of the reboiler and one to represent the dynamics of the column, and six algebraic equations. The method outlined for obtaining the reduced model can be extended for systems with more than four components by similar lumping approaches.

The reduced model when used in a nonlinear model predictive controller algorithm gives tight control of the system. The performance of the controller with the reduced model is comparable to the performance with the detailed column model in the control algorithm, with an added advantage of reduced computational effort. The NLMPC algorithm calculates the inputs to give the desired amount of distillate. Constraints on the temperature of tray 2, which is sensitive to the changes in the system, ensure that the purity of the distillate collected is within specified bounds.

Large nonlinear optimization problems have presented a considerable challenge for reliable application of nonlinear MPC. One method to address feasibility and robustness of such approaches is to minimize the computational complexity by using a reduced order fundamental model of the type described in this paper.

Acknowledgements

The authors would like to thank Dr. Ramkrishna and R.M. Wajge at Purdue University for helpful discussions.

References

[1] M.F. Doherty, G. Buzad, Reactive distillation by design, Chem. Eng. Res. Des. 70 (1992) 448–458.
[2] D. Barbosa, M.F. Doherty, The simple distillation of homogeneous reactive mixtures, Chem. Eng. Sci. 43 (1988) 541–550.
[3] D. Barbosa, M.F. Doherty, The influence of equilibrium chemical reactions on vapor–liquid phase diagrams, Chem. Eng. Sci. 43 (1988) 529–540.
[4] M.F. Doherty, G. Buzad, New tools for the design of kinetically controlled reactive distillation columns, Comput. Chem. Engng. 18 (Suppl.) (1994) S1–S13.
[5] J. Espinosa, P.A. Aguirre, G.A. Perez, Product composition regions of single-feed reactive distillation columns: mixtures containing inerts, Ind. Eng. Chem. Res. 34 (1995) 853–861.
[6] V. Julka, M.F. Doherty, Geometric nonlinear analysis of multicomponent nonideal distillation: a simple computer-aided design procedure, Chem. Eng. Sci. 48 (1993) 1367–1391.
[7] K. Alejski, Computation of the reacting distillation column using a liquid mixing model on the plates, Comput. Chem. Engng. 15 (1991) 313–323.
[8] M.A. Isla, H.A. Irazoqui, Modeling, analysis, and simulation of a methyl *tert*-butyl ether reactive distillation column, Ind. Eng. Chem. Res. 35 (1996) 2696–2708.
[9] R. Paludetto, G. Paret, G. Donati, Multicomponent distillation with chemical reaction mathematical model analysis, Chem. Eng. Sci. 47 (1992) 2891–2896.
[10] P.R. Senthilnathan, P.G. Sriram, S.K. Ghosh, Computations for multistage multicomponent separation involving chemical and ionic equilibria and reactions, The Chem. Eng. J. 37 (1988) 93–106.
[11] J. Simandi, W.Y. Svrcek, Extension of the simultaneous-solution and inside–outside algorithms to distillation columns with chemical reactions, Comput. Chem. Engng. 15 (1991) 337–348.
[12] A.R. Ciric, P. Miao, Steady state multiplicities in an ethylene glycol reactive distillation column, Ind. Eng. Chem. Res. 33 (1994) 2738–2748.
[13] R. Jacobs, R. Krishna, Multiple solutions in reactive distillation for methyl *tert*-butyl ether synthesis, Ind. Eng. Chem. Res. 32 (1993) 1706–1709.
[14] S.A. Nijhuis, F.P.J.M. Kerkhof, A.N.S. Mak, Multiple steady states during reactive distillation of methyl *tert*-butyl ether, Ind. Eng. Chem. Res. 32 (1993) 2767–2774.
[15] A.A. Abufares, P.L. Douglas, Mathematical modeling and simulation of an MTBE catalytic distillation process using SPEEDUP and ASPENPLUS, Int. Chem. Eng. 73 (1995) 3–12.
[16] J.H. Grosser, M.F. Doherty, M.F. Malone, Modeling of reactive distillation systems, Ind. Eng. Chem. Res. 26 (1987) 983–989.
[17] M. Savkoviý-Stevanović, M. Mišić-Vukovič, G. Bončic-Carićić, B. Trišovic, S. Jezdić, Reactive distillation with ion exchangers, Separation Science and Technology 27 (1992) 613–630.
[18] S. Schrans, S.D. Wolf, R. Baur, Dynamic simulation of reactive distillation: an MTBE case study, Comput. Chem. Engng. 20 (1996) S1619–S1624.
[19] P.E. Cuille, G.V. Reklailis, Dynamic simulation of multicomponent batch rectification with chemical reactions, Comput. Chem. Engng. 10 (1986) 389–398.
[20] E. Reuter, G. Wozny, L. Jeromin, Modeling of multicomponent batch distillation processes with chemical reaction and their control systems, Comput. Chem. Engng. 13 (1989) 449–510.
[21] E. Sørensen, S. Skogestad, Control strategies for reactive batch distillation, J. Proc. Cont. 4 (1994) 205–217.
[22] R.M. Wajge, G.V. Reklaitis, Campaign optimization of multicomponent reactive batch distillation, AIChE Spring Meeting, New Orleans, LA, 1996.
[23] R.M. Wajge, R.V. Reklaitis, Design of optimal reflux policy for multicomponent reactive distillation in packed bed, AIChE Annual Meeting, Miami, FL, 1995.
[24] A. Kumar, P. Daoutidis, A DAE framework for modeling and control of reactive distillation columns, in Symposium on Dynamics and Control of Chemical Reactors, Distillation Columns, and Batch Processes, IFAC, 1995.

[25] A. Kumar, P. Daoutidis, Nonlinear control of a high-purity ethylene glycol reactive distillation column, in: IFAC Symposium on Advanced Control of Chemical Processes, 1997, pp. 371–376.
[26] J.L. Baldon, J.J. Strifezza, M.S. Basualdo, C.A. Ruiz, Control policy for the startup, semi-continuous and continuous operation of a reactive distillation column, in: IFAC Symposium on Advanced Control of Chemical Processes, 1997, pp. 125–130.
[27] M.H. Bassett, P. Dave, F.J. Doyle III, G.K. Kudva, J.F. Pekny, G.V. Reklaitis, Perspectives on model based integration of process operations, Comput. Chem. Engng. 20 (1996) 821–844.
[28] M. Morari, E. Zafiriou, Robust Process Control, Prentice Hall, Englewood Cliffs, NJ, 1989.
[29] Y.L. Hwang, Nonlinear wave theory for dynamics of binary distillation columns, AIChE J. 37 (1991) 705–723.
[30] Y.L. Hwang, On the nonlinear wave theory for dynamics of binary distillation columns, AIChE J. 41 (1995) 190–194.
[31] W. Marquardt, Traveling waves in chemical processes, Int. Chem. Eng. 30 (1990) 585–606.
[32] W.L. Luyben, Profile position control of distillation columns with sharp temperature profiles, AIChE J. 18 (1972) 238–240.
[33] A.S. Bostandzhiyan, A.A. Butakov, K.G. Shkadinskii, Critical conditions and waves for exothermic processes in fixed-bed catalytic reactors, Theor. Found. Chem. Eng. 23 (1989) 36–41.
[34] J. Puszyński, V. Hlavacek, Experimental study of ignition and extinction waves and oscillatory behavior of a tubular nonadiabatic fixed bed reactor for the oxidation of carbon monoxide, Chem. Eng. Sci. 39 (1984) 681–692.
[35] F.G. Helfferich, G. Klein, Multicomponent Chromatography: Theory of Interference, Marcel Dekker, New York, 1970.
[36] Y.L. Hwang, F.G. Helfferich, Dynamics of continuous countercurrent mass-transfer processes: III multicomponent systems, Chem. Eng. Sci. (1989) 44.
[37] H Rhee, R. Aris, N.R. Amundson, First-order partial differential equations: theory and application of hyperbolic systems of quasilinear equations, vol. 2. Prentice Hall, Englewood Cliffs, NJ, 1986.
[38] L.S. Balasubramhanya, F.J. Doyle III, Nonlinear control of a high-purity distillation column using a traveling wave model, AIChE J. 43 (1997) 703–714.
[39] F.J. Doyle III, H.M. Budman, M. Morari, Linearizing controller design for a packed-bed reactor using a low-order wave propagation model, Ind. Eng. Chem. Res. 35 (1996) 3567–3580.
[40] H. Han, S. Park, Control of high-purity distillation column using a nonlinear wave theory, AIChE J. 39 (1993) 787–796.
[41] M. Han, S. Park, Startup of distillation columns using nonlinear wave model based control, in: IFAC Symposium on Advanced Control of Chemical Processes, 1997, pp. 616–622.
[42] W. Marquardt, E.D. Gilles, Nonlinear wave phenomena as fundamentals for model based control system design in distillation, AIChE Annual Meeting, Chicago, IL, 1990.
[43] L.S. Balasubramhanya, Low order models for nonlinear process control, PhD thesis, Purdue University, August 1997.
[44] S.J. Qin, T.A. Badgwell, An overview of industrial model predictive control technology, in: Proceedings of the Fifth International Conference on Chemical Process Control, Tahoe City, CA, 1996 (preprint).
[45] N.L. Ricker, Model predictive control with state estimation, Ind. Eng. Chem. Res. 29 (1990) 374–382.